Antiviral Research 80 (2008) 360–369

Contents lists available at ScienceDirect

Antiviral Research

journal homepage: www.elsevier.com/locate/antiviral

# A scintillation proximity assay for dengue virus NS5 2′-*O*-methyltransferase—kinetic and inhibition analyses

Siew Pheng Lim[a,*], Daying Wen[a], Thai Leong Yap[b], Chung Ka Yan[b], Julien Lescar[b], Subhash G. Vasudevan[a,1]

[a] *Novartis Institute for Tropical Diseases, 10 Biopolis Road, #05-01 Chromos, Singapore 138670, Singapore*
[b] *School of Biological Sciences, Nanyang Technological University, 60, Nanyang Drive, Singapore 637551, Singapore*

ARTICLE INFO

*Article history:*
Received 2 June 2008
Received in revised form 18 August 2008
Accepted 25 August 2008

*Keywords:*
Dengue
Methyltransferase
Assay
Kinetics
Compound
Inhibition

ABSTRACT

Dengue virus (DENV) NS5 possesses methyltransferase (MTase) activity at its N-terminal amino acid sequence and is responsible for formation of a type 1 cap structure, $m^7GpppAm^{2'-O}$ in the viral genomic RNA. Optimal *in vitro* conditions for DENV2 2′-*O*-MTase activity were characterized using purified recombinant protein and a short biotinylated GTP-capped RNA template. Steady-state kinetics parameters derived from initial velocities were used to establish a robust scintillation proximity assay for compound testing. Pre-incubation studies showed that MTase–AdoMet and MTase–RNA complexes were equally catalytically competent and the enzyme supports a random bi bi kinetic mechanism. The assay was validated with competitive inhibitory agents, *S*-adenosyl-homocysteine and two homologues, sinefungin and dehydrosinefungin. A GTP-binding pocket present at the N-terminal of DENV2 MTase was previously postulated to be the cap-binding site. Interestingly, inhibition of the enzyme by GTP was two-fold lower than with RNA cap analogues, G[5′]ppp[5′]A and $m^7$G[5′]ppp[5′]A and about three-fold poorer than a two-way methylated analogue, $m^7$G[5′]ppp[5′]$m^7$G. This assay allows rapid and highly sensitive detection of 2′-*O*-MTase activity and can be readily adapted for high-throughput screening for inhibitory compounds. It is suitable for determination of enzymatic activities of a wide variety of RNA capping MTases.


## 1. Introduction

Dengue and dengue hemorrhagic fever (DF/DHF) are the most frequent arthropod transmitted infectious diseases in humans and are endemic in the tropics and subtropics. They are caused by one of four closely related, but antigenically distinct, dengue virus serotypes (DENV-1 to -4), of the genus *Flavivirus* (reviewed in Gubler, 1998). Genomes of DENV, like other members of the *Flavivirus* family (Lindenbach and Rice, 2001), consist of a single positive-stranded RNA of approximately 11 kb, with a type 1 cap structure $m^7GpppAm^{2'-O}G$ (Chambers et al., 1990) where the first two nucleotides are strictly conserved (Cleaves and Dubin, 1979; Wengler, 1981). The RNA consists of a 5′ and 3′-untranslated region (UTR) encompassing a single long open reading frame (Rice et al., 1985) which encodes three structural proteins and seven non-structural proteins (Lindenbach and Rice, 2001). The role of the cap structure is to protect viral RNA from degradation by host endonucleases and to enhance translation initiation (Furuichi and Shatkin, 2000; Shuman, 2001; Gu and Lima, 2005). Of the four enzymes known to be involved in formation of DENV cap 1 structure (reviewed in Shuman, 2001), the RNA triphosphatase has been mapped to NS3 (Li et al., 1999) whilst the N7- (Ray et al., 2006; Dong et al., 2007; Zhou et al., 2007) and 2′-*O*- (Egloff et al., 2002) methyltransferase (MTase) activities are encoded in NS5. The guanylyltransferase has not been identified.

DENV MTase domain is located at amino acid residues 1–296 of NS5 (Egloff et al., 2002) and is conserved across the *Flavivirus* family (Koonin, 1993). Interestingly, a novel guanosine 5′-tri-phosphate (GTP)-specific binding site is found at its N-terminal sequence (Egloff et al., 2002). Co-complexed DENV MTase crystal structures with RNA cap analogues and *S*-adenosyl-homocysteine (SAH) showed that it corresponds to the GTP cap-binding site (Egloff et al., 2007). Ribavirin 5′-triphosphate (RTP), GTP or RTP analogues and

*Abbreviations:* AdoMet, *S*-adenosyl-L-methionine; DENV, dengue virus; DENV2, dengue virus type 2; DF/DHF, dengue fever/dengue hemorrhagic fever; DTT, dithiothreitol; DNMT, DNA methyltransferase; $IC_{50}$, inhibitory concentration that causes 50% reduction in enzyme activity; IPTG, isopropanol-D-thiogalactopyranoside; kan, kanamycin; LB, Luria-Bertani broth; MTase, methytransferase; NS, non-structural; PCR, polymerase chain reaction; RTP, ribavirin triphosphate; RdRp, RNA-dependent RNA polymerase; SAH, *S*-adenosyl-L-homocysteine; SAM, *S*-adenosyl-L-methionine; TAP, tobacco acid pyrophosphatase; Tm, melting temperature; WNV, West Nile virus.

* Corresponding author. Tel.: +65 6722 2924; fax: +65 6722 2916.
*E-mail address:* siew_pheng.lim@novartis.com (S.P. Lim).
[1] Present address: School Emerging Infectious Diseases Program, Duke-NUS Graduate Medical School, Singapore 169547, Singapore.

0166-3542/$ – see front matter © 2008 Elsevier B.V. All rights reserved.
doi:10.1016/j.antiviral.2008.08.005

RNA cap analogues can bind at this site and inhibit enzyme activity (Benarroch et al., 2004; Egloff et al., 2007).

Both N7- and 2′-*O*-MTase activities from West Nile virus (WNV) NS5 have been extensively studied (Ray et al., 2006; Dong et al., 2007; Zhou et al., 2007). They act in sequential order with 2′-*O* taking place after re-positioning of the N7-methylated cap structure into the GTP-binding pocket (Dong et al., 2008). Distinct amino acids within the $K_{61}D_{146}K_{182}E_{218}$ motif and the RNA binding pocket are responsible for either or both activities, whilst residues in the GTP-pocket were found to be important for mediating 2′-*O* activity. Furthermore, N7-MTase activity requires RNA templates with a 5′ stem-loop structure spanning at least 74 nt of the viral 5′ UTR with specific nucleotides at the 2nd and 3rd positions, whilst 2′-*O*-MTase activity functions on short RNA templates with specific nucleotides at the 1st and 2nd positions (Dong et al., 2007). Intriguingly, unlike cellular cap MTases which are not sequence-specific (Mao et al., 1995), flavivirus cap methylation is specific for their cognate viral RNA sequence as no MTase activity was detected on capped RNA derived from plasmid sequences nor on viral 5′ UTR with mutations in the first 4 nt (Dong et al., 2007).

Abolishment of WNV N7-MTase activity inhibited virus replication in cells, whilst that of 2′-*O*-MTase activity attenuated virus growth only in cells (Ray et al., 2006) and mice (Zhou et al., 2007). Similarly, we have observed that mutations in both GTP and *S*-adenosylmethionine (SAM) binding pockets severely affected DENV2 MTase enzymatic activity and abolished viral replication in cells (Kroschewski et al., 2008). This makes MTase a promising drug target for inhibition of *Flavivirus* related diseases. On that note, the homologue of AdoMet, sinefungin (Smith and Norton, 1980; Chrebet et al., 2005) which has been reported to have anti-fungal, anti-protozoal and anti-viral activities (Pugh et al., 1978; Ghosh and Liu, 1997) was found to inhibit WNV replication (Dong et al., 2008). Interestingly, the physical organization of subunit components, structure and catalytic mechanisms of Flavivirus capping enzyme differs significantly from other host and viral RNA MTases, suggesting that it may be possible to generate inhibitors that are selective to Flavivirus MTases (Egloff et al., 2002). An effort to find specific inhibitors to DENV MTase has been undertaken by Luzhkov et al. (2007) using a high-throughput virtual screening approach. An inhibitor with an $IC_{50}$ value of 60 μM was identified using a filter-based assay following testing of the top 15 ranking compounds. Nevertheless, this assay format is not compatible with large-scale compound screening and also requires relatively large amounts of protein and RNA.

To better understand the enzymatic characteristics of DENV 2′-*O*-MTase, and to develop a robust assay that is suitable for testing large numbers of compounds, we expressed the recombinant form of DENV2 MTase protein and determined the optimal *in vitro* conditions for its activity. We next performed kinetic analyses to determine the steady-state kinetic parameters for methylation and further developed a streptavidin bead-based scintillation proximity assay (SPA) to evaluate the inhibitory properties of various competitive and non-competitive agents.

## 2. Materials and methods

### 2.1. Materials

RNA substrate, 5′-GpppAGAACCUG-biotin-TEG-3′ was chemically synthesized. *S*-Adenosyl-L-methionine chloride (SAM) and *S*-adenosyl-homocysteine (SAH) were purchased from Sigma (St. Louis, MO). GTP and recombinant RNasin® Ribonuclease Inhibitor (40 U/μl) were ordered from Promega (Madison, WI). *S*-Adenosyl-L-[methyl-$^3$H]-methionine (72 Ci/mmol) and streptavidin-coated SPA beads were purchased from Amersham Biosciences (Piscataway, NJ). Competent M15 (pREP4) were obtained from Qiagen (Valencia, CA). RNA cap analogues, m$^7$G[5′]ppp[5′]A and G[5′]ppp[5′]A were purchased from NEB (Ipswich, MA), $m_{2,3'\text{-}O}^{7}$G[5′]ppp[5′]G, $m_2^{2,2,7}$G[5′]ppp[5′]G, m$^7$G[5′]ppp[5′]m$^7$G were purchased from Epicentre Biotechnologies (Madison, WI).

### 2.2. Cloning of DENV2 TSV01 NS5 MTase

The gene encoding the N-terminal part of the NS5 cDNA comprising amino acids 1–296 was amplified by PCR using Pfu polymerase (Stratagene, La Jolla, CA) with the forward (5′-CAC *GGA TCC* GGA ACT GGC AAC ACA GGA GAG-3′) and reverse primers (5′-CTG CAG *GTC GAC* TTA TTG GTC ATA GTG CCA TGA-3′) and the template pET15b-NS5 (aa 1–900) from DENV2 isolate TSV01 (accession no. AY037116). Underlined sequences correspond to BamHI and SalI sites, respectively. PCR conditions were: 94 °C for 5 min; followed by 30 cycles of 94 °C for 1 min, 55 °C for 1 min and 72 °C for 1 min; and 72 °C for 10 min. The resultant PCR product was digested with BamHI and SalI, and ligated into the same sites in pQE30 (Qiagen, Valencia, CA) using Roche Rapid DNA ligation kit (Base, CH) to generate the construct pQE30-DENV2 MTase. The ligation mixture was transformed into XL1BLUE cells (Stratagene) and positive clones were isolated and the sequence of the constructs was verified by automated nucleotide sequencing (PerkinElmer Applied Biosystems, Foster City, CA).

### 2.3. Expression and purification of DENV2 MTase

Competent M15 (pREP4; Stratagene) were transformed with pQE30-DENV2 MTase and grown overnight on Luria-Bertani (LB; 100 μg/ml ampicillin, 10 μg/ml kanamycin) plates. A single colony was re-suspended in 5 ml LB, grown overnight at 37 °C, followed by inoculation into 500 ml LB media (100 μg/ml ampicillin, 10 μg/ml kanamycin) and incubation with shaking (220 rpm) at 37 °C until $OD_{595} \sim 0.5$. Cultures were induced with 0.4 mM IPTG and growth was continued for a further 5 h at 30 °C. The resulting cells were again pelleted by centrifugation as before and each liter was re-suspended in 15 ml cold buffer A (50 mM Bicine pH 7.5, 300 mM NaCl, 5 mM imidazole, 10% (v/v) glycerol). Cells were sonicated and the debris was removed by centrifugation at 50,000 × *g* for 30 min. The protein solution was then loaded onto a 5 ml HiTrap chelating HP (Amersham Biosciences) column equilibrated with buffer A (flow-rate: 1 ml/min). The column was washed with 5 column volume buffer A and protein eluted from the column with buffer A and a linear gradient concentration of imidazole from 5 to 500 mM (flow-rate: 1 ml/min). The peak fractions were analysed by 12% SDS PAGE. A second purification step consisted of cation-exchange chromatography (SP-Sepharose; Amersham Biosciences) in 50 mM Bicine buffer, pH 7.5, 1 mM dithiothreitol (DTT), 10% glycerol, applying a salt gradient from 0.15 to 1.5 M NaCl. DENV2 MTase eluted around 1 M NaCl. After concentration by ultra-centrifugation with Amicon spin columns, molecular weight cut-off = 10,000 Da), a final step using gel-filtration chromatography (Superdex-20010/300GL; Amersham Biosciences) was performed in 50 mM Bicine, pH 7.5, 0.8 M NaCl, 1 mM DTT and 10% glycerol. The monomeric protein was concentrated as before up to 25 mg/ml and used for characterization.

### 2.4. DENV2 2′-O-MTase assay and enzyme characterization

To determine the optimal conditions for the assay, various parameters were tested. Assays were carried out at 37 °C, 30 °C or RT for 0–3 h in a total volume of 25 μl with 10–100 nM enzyme and 4–20 mg/ml streptavidin-coated SPA beads. Amount of RNA substrate tested ranged from 40 to 100 nM, and that of [methyl-

$^3$H]-AdoMet varied from 0.5 to 2 μCi (or 0.28 to 1.12 μM). For enzyme characterization, pH dependence was determined over a range from 6 to 10 using 50 mM MES (pH 6.0), MOPS (pH 6.5), and Tris/HCl (pH 7, 7.5, 8, 8.5, 9, 9.5 and 10) with 2 mM DTT and 5 U RNasin®. The effects of 0–300 mM NaCl, 10 mM KCl, 2 mM $MgCl_2$, 2 mM $MnCl_2$ and 0–0.05% (w/v) CHAPS were assessed at pH 7–10. To set up the reaction, the buffer, template and enzyme were first mixed together in a single well in a 96-well 1/2 area, white opaque plates (Corning Costar, Acton, MA) and [methyl-$^3$H]-AdoMet added last. The reaction was stopped with 25 μl of 2× stop solution (100 mM Tris/HCl, pH 7, 100 mM EDTA, 600 mM NaCl, 4 mg/ml streptavidin–SPA beads and 62.5 μM cold AdoMet) and shaken for 20 min at 750 rpm at room temperature followed by centrifugation for 2 min at 1200 rpm. The plate was read in a Trilux microbeta counter (PerkinElmer, Boston, MA) with a counting time of 1 min/well. All data points were measured in duplicate. The final assay buffer contained 50 mM Tris/HCl, pH 7.0, 10 mM KCl, 2 mM $MgCl_2$, 2 mM $MnCl_2$, 0.05% (v/v) CHAPS, 2 mM DTT, and 5 U RNasin® inhibitor.

### 2.5. Determination of kinetic parameters

Two sets of experiments were performed in the final assay buffer with either 25 nM enzyme, 0.95 μM [methyl-$^3$H]-AdoMet and RNA substrate concentration varying from 0 to 0.5 μM or with 25 nM enzyme, 2 μM RNA substrate and [methyl-$^3$H]-AdoMet concentration varying from 0 to 1 μM. Total reaction time was 20 min. All data points were done in duplicate, plotted as Michaelis–Menten graphs for velocity as function of either RNA or AdoMet concentrations using GraphPad Prism® version 3.02 program (GraphPad Software, Inc.). At least two independent experiments were performed for each set of experiments. Since the reactions were performed at constant enzyme concentration with one substrate always at saturating amounts whilst the concentration of the other substrate is varied, the kinetic parameter $K_m$ is equal to the Michaelis constant and both $K_m$ and $V_{max}$ may be obtained after nonlinear regression curve fitting according to Eq. (1). $k_{cat}$ was calculated as the ratio of $V_{max}$ to enzyme concentration used. Product formation was measured as count/min. The final nanomolar product formed ($N$; [$^3$H] $CH_3$ group transfer) was calculated as $P = [(Y - B)/E] \times F$, where $Y$ is counts/min for each experiment, $B$ is counts/min of blank, $E$ is counting efficiency (0.57), $F$ is counts/min/nM free [$^3$H]-AdoMet. Product formed per min was obtained as $N/T$, where $T$ is the time of reaction (20 min). The rate of product formation ($v$, nM min$^{-1}$) was plotted against substrate concentration and fitted into one site binding equation as follows

$$v = \frac{V_{max}^{app}[S]}{K_m^{app}[S]} \quad (1)$$

where $V_{max}^{app}$ corresponds to maximal velocity and $K_m^{app}$ is the substrate concentration needed to reach half-maximal velocity. From $V_{max}^{app}$, turnover number ($k_{cat}$) was calculated as: $k_{cat} = V_{max}/[E_t]$, where $E_t$ defines the total concentration of enzyme. Double reciprocal plots of initial velocity ($1/v$) versus concentrations of RNA substrate or [methyl-$^3$H]-AdoMet were also plotted on Lineweaver-Burk double reciprocal plots and fitted to weighted linear regression. Initial velocity $1/v$ was obtained as $E_t \times T/N$.

### 2.6. Pre-incubation studies

Pre-incubation experiments were carried out by incubating 25 nM DENV2 MTase with either 1 μCi [methyl-$^3$H]-AdoMet (0.56 μM) or 40 nM RNA substrate for 10 min at RT. Reaction was started by adding the missing reactant, either RNA substrate or [methyl-$^3$H]-AdoMet, respectively. At every 10 min intervals, 25 μl of reaction was stopped with 2× stop buffer and the counts determined as described earlier. In a control experiment, [methyl-$^3$H]-AdoMet and RNA substrate were similarly pre-incubated for 10 min at room temperature and the reaction started with the addition of DENV2 MTase.

### 2.7. Treatment of RNA substrate with tobacco acid pyrophosphatase

A master tube containing 10 pmoles of RNA substrate was incubated with 250 nM DENV2 MTase and 10 μCi [methyl-$^3$H]-AdoMet for 1 h at RT, after which the RNA was recovered by extraction with phenol:chloroform:isoamyl alcohol and precipitation with ethanol. Half of the RNA substrate was then treated with 5 U tobacco acid pyrophosphatase (TAP) in 50 mM sodium acetate, pH 6, 1 mM EDTA, 0.1% beta-mercaptoethanol and 0.01% Triton-X-100 (Epicentre Biotechnologies) for 2 h at 37 °C, whilst the remaining half was similarly incubated but in buffer without enzyme. Equal volumes of 2× stop buffer were added to both samples and these were shaken for 20 min, spun down and quantified as before on the microbeta counter.

### 2.8. Treatment of RNA substrate with vaccinia virus N7- and 2′-O-methyltransferases

A master tube containing 10 pmoles of RNA substrate was incubated with 0.1 mM cold AdoMet in 50 mM Tris/HCl, pH 8, 6 mM KCl and 1.25 mM $MgCl_2$ in the presence or absence of 5 U vaccinia virus N7-methyltransferase (Epicentre Biotechnologies) for 1 h at 37 °C, after which the RNA samples were recovered by extraction with phenol:chloroform:isoamyl alcohol and precipitation with ethanol. Thereafter, they were treated with 62.5 nM DENV2 MTase and 2 μCi [methyl-$^3$H]-AdoMet for 1 h at RT, followed by addition of equal volumes of 2× stop buffer. Alternatively, four master tubes containing 4 pmoles of RNA substrate were incubated with 0.1 mM cold AdoMet in 50 mM Tris/HCl, pH 8, 6 mM KCl and 1.25 mM $MgCl_2$ in the absence of enzymes or presence 5 U vaccinia virus N7-methyltransferase, 2′-O-methyltransferase, or N7- and 2′-O-methyltransferases, for 2 h at 37 °C, after which the RNA samples were ethanol precipitated as before. Thereafter, each tube was separately treated with 50 nM DENV2 MTase and 2 μCi [methyl-$^3$H]-AdoMet for 1 h at RT, followed by addition of equal volumes of 2× stop buffer. All samples were shaken for 20 min and quantified as before on the microbeta counter.

### 2.9. Inhibitor testing

Unless otherwise stated, all compounds were tested at a maximum concentration of 20 μM with two-fold serial dilutions. Inhibitors were assayed in a 96-well plate format in a final volume of 25 μl in 50 mM Tris/HCl, pH 7.0, 10 mM KCl, 2 mM $MgCl_2$, 2 mM $MnCl_2$, 0.05% (v/v) CHAPS, 2 mM DTT, and 5 U RNasin® inhibitor. Typically 25 nM enzyme and 40 nM RNA substrate were pre-incubated with various concentrations of test compounds at room temperature for 30 min. The reaction was then initiated by addition of 0.56 μM [methyl-$^3$H]-AdoMet and allowed to continue for 20 min. The reaction was stopped with 2× stop solution as described before and the plates read. All data points were measured in duplicate. $K_i$ values were determined by fitting the calculated initial velocities (counts/min) to a nonlinear regression curve fit using GraphPad Prism® software. Unless stated, kinetic experiments were designed on the basis of the methodology described by Copeland (2000).

### 2.10. Data analysis

Data were analysed on a plate-by-plate basis. $Z'$ factor which represents the quality assessment of the assay during development and optimization (Zhang et al., 1999) was calculated for each plate using the average counts obtained with wells as positive control (no compound added) and negative control (no RNA substrate added). Readings were averaged for each duplicate concentration of compound tested and the raw values plotted as average counts/min against the log of compound concentration. The standard deviation is calculated by the non-biased $n-1$ method, S.D. = $\sqrt{((n\Sigma x^2 - (\Sigma(x)^2)/(n(n-1)))}$. Nonlinear regression (curve fit) and the equation for sigmoidal dose–response (variable slope) from GraphPad Prism® were used to interpolate values for $IC_{50}$ values. The equation is as follows:

$$Y = \frac{\text{Bottom} + (\text{Top} - \text{Bottom})}{1 + 10^{[(\log EC_{50} - X) \times \text{Hill Slope}]}}$$

where $X$ is the logarithm of concentration. $Y$ is the response; $Y$ starts at Bottom and goes to Top with a sigmoid shape.

This is identical to the "four parameter logistic equation" (Rodbard and Hutt, 1974; Finney, 1976).

## 3. Results and discussion

### 3.1. Expression, purification and characterization of DENV2 MTase

Expression of recombinant DENV2 MTase as a N-terminal His-tag fusion protein in *Escherichia coli* led to the production of a highly soluble protein. Following affinity chromatography on $Ni^{2+}$ columns, >95% of the protein obtained was full length, with a molecular weight of about 34 kDa (Fig. 1A). Some minor proteolysis occurred, giving rise to a truncated product (Fig. 1A, lanes 4–6). The protein was further purified through ion exchange and gel filtration chromatography and the monomeric fractions (>95% purity) were pooled together and further concentrated (Fig. 1B). The final yield was 4 mg of protein per litre of culture. The protein was stored at −80 °C and could be left at room temperature for an hour (Supplementary Fig. 1A) or frozen–thawed more than 10 times (data not shown) without any loss in activity.

Recombinant DENV2 MTase was assayed for optimal buffer conditions with respect to pH, cations, detergent and temperature using a short biotinylated RNA template in a scintillation proximity assay (Wu and Liu, 2000). We first performed a time course experiment to determine MTase activity at different pH ranging from 6 to 10 (Fig. 2A). The enzyme displayed very poor activity at pH 6–7 even after prolonged incubation of 1 h. When the pH of the buffer was increased from 7.5 to 10, a proportional increase in enzymatic activity was observed. This was detected as early as 10 min after initiation and continued to rise linearly over the 1-h period. Maximum activity (corresponding to 7.16 ± 0.45 nM of RNA methylated) was detected at pH 10 after 1 h. This requirement for high pH for catalytic activity is likely a consequence of the high p$K_a$ of K182 (free Lys has p$K_a$ value = 10.5) which participates in the deprotonation of ribose 2′-OH (p$K_a$ = 12.5) from the AdoMet moiety bound in the MTase catalytic site (Dong et al., 2007). Similar requirements for high pH for methylation have been reported for WNV MTase (Dong et al., 2007; Zhou et al., 2007) and human guanine N7-MTase (Ogino et al., 2005).

Next, the enzyme was incubated for 20 min in the same buffers from pH 6 to 10 in the presence of various cations. We had previously observed that DENV full length NS5 and the polymerase domain were optimally active in the presence of 10 mM KCl, 2 mM $MgCl_2$ and 2 mM $MnCl_2$ (Yap et al., 2007). To assess if DENV MTase domain had similar properties, we tested our protein in the presence of these cations. Controls without cations were first assayed again for 20 min (Fig. 2B). As was observed before, no enzymatic activity was observed at pH 6–9.5 whilst very low levels of methylation occurred at pH 10. Addition of 10 mM KCl resulted in detectable enzymatic activity at pH 8–10 (Fig. 2B). Although the activity was highest at pH 10 (3.1 nM RNA methylated), maximum enhancement in activity was detected at pH 8.5 (from 0 to 1.9 ± 0.3 nM RNA methylated). Addition of 2 mM $MgCl_2$ led to a significant increase in activity from pH 7 to 10 (Fig. 2B). Both the highest activity and maximum enhancement were observed at pH 8.5 and 9 (approximately 15.2 nM RNA methylated). Interestingly, addition of 2 mM $MnCl_2$ produced a completely different profile, with enhanced activity present only between pH 7 and 8 and very low or negligible levels of activity observed at pH 6, 8.5 and 9–10 (Fig. 2B). Maximum activity occurred at pH 7.5 with about 12.5 nM RNA methylated.

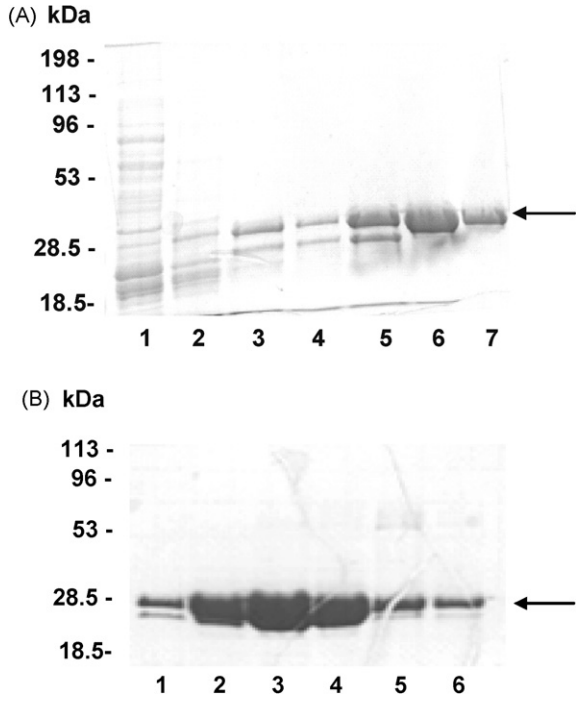


**Fig. 1.** Expression and purification of recombinant DENV2 MTase. SDS-PAGE analysis of DENV2 MTase after purification through $Ni^{2+}$ affinity column (A). Lane 1 consists of pre-stained protein marker, lane 2, flow through, and lanes 3–9 are the purified protein fractions pooled for a second round of purification. Protein purity is about 95% with some proteolysis (lanes 4–6). SDS-PAGE analysis of DENV2 MTase after purification through ion-exchange and gel filtration (monomeric fraction) chromatography (B). Lane 1 consists of pre-stained protein marker, lanes 2 and 3 are fractions of aggregated protein, lanes 4–8 are monomeric fractions which were pooled together and concentrated for activity tests. Protein purity was about 95%. Arrows indicate purified protein with molecular weight of 34 kDa.

Both $MgCl_2$ and $MnCl_2$ had significantly stronger stimulatory effects on the enzyme compared to KCl. In addition, both divalent cations induced a bell-shaped profile albeit with different pH maximal for activity. The reason for this is unclear, although a similar profile has been observed for vaccinia virus 2′-*O*-MTase, VP39 (Li and Gershon, 2006). Nevertheless, there may be several possible reasons for the observed enhancement of enzymatic activity by the cations: they could (i) decrease the p$K_a$ of either K182 and/or ribose 2′-OH and shift it closer to neutral pH, (ii) decrease $K_m$ of RNA by stabilizing the RNA through reducing electrostatic repulsion of its phosphate groups and/or (iii) decrease $K_m$ of AdoMet. The first reason would result in a higher catalytic activity of the enzyme and the latter two would increase binding affinity of the substrate(s).

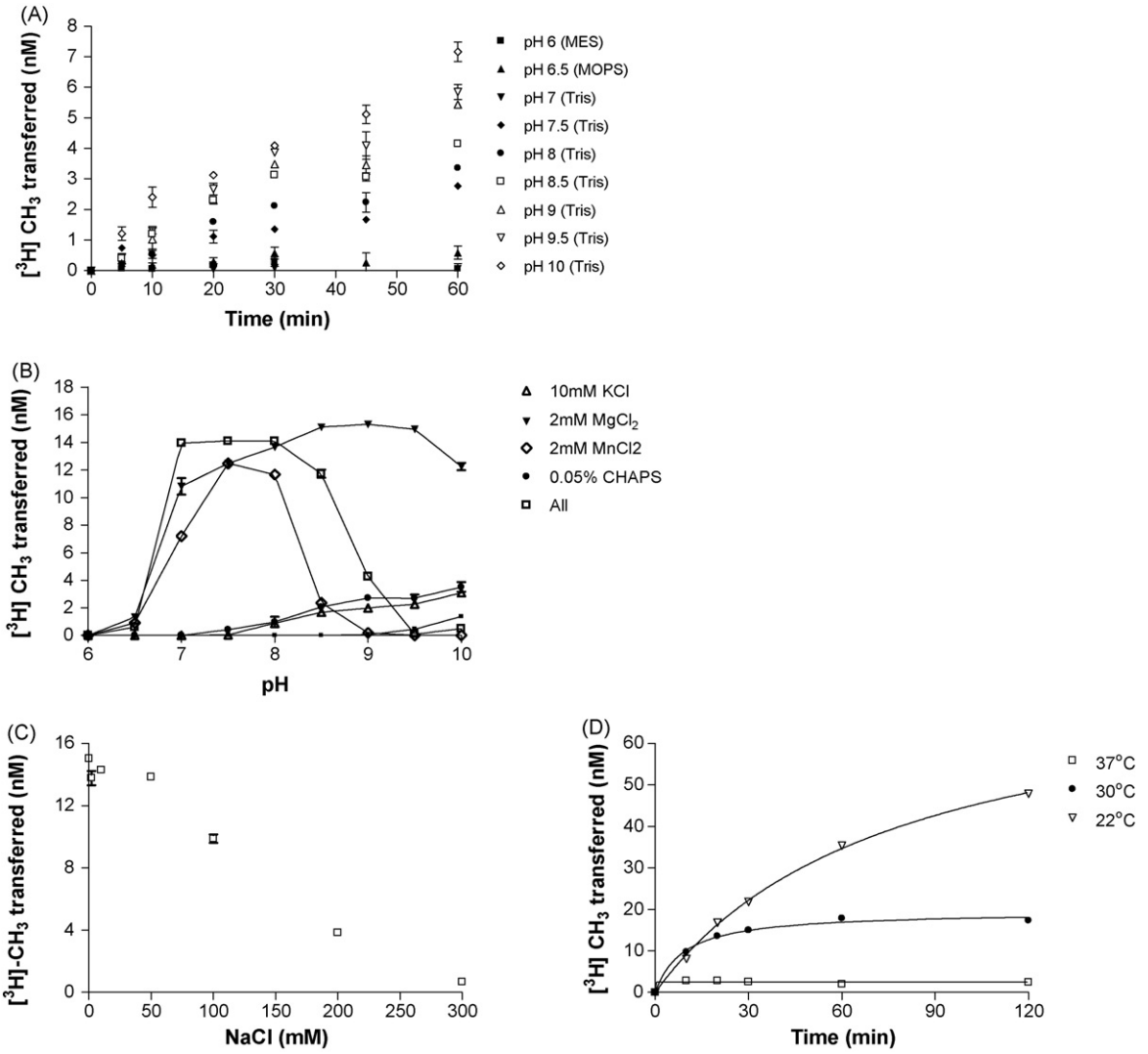


**Fig. 2.** Determination of optimal buffer conditions for DENV2 MTase activity. 25 nM of MTase was tested against 40 nM RNA substrate and 0.56 μM [methyl-$^3$H]-AdoMet in all assays. pH dependence of enzymatic activity using different buffers in the pH range from 6 to 10.0 (MES, pH 6.0; MOPS, pH 6.5, and Tris/HCl, pH 7.0–10) was performed over 1 h period (A) or for 20 min (B) at RT. Effects of 10 mM KCl (open triangle), 2 mM $MgCl_2$ (inverted closed triangle), 2 mM $MnCl_2$ (open diamond) 0.05% CHAPS (closed circle) alone or in combination (open square) on activity of MTase was tested at pH 6–10 with a total reaction time of 20 min. Effect of ionic strength on MTase activity was tested at pH 7 in the presence of 10 mM KCl, 2 mM $MgCl_2$, 2 mM $MnCl_2$ and 0.05% CHAPS, for 20 min with 0, 2, 10, 100 or 300 mM NaCl (B). Effect of temperature on MTase activity was evaluated at 22, 30 and 37 °C over a period of 2 h with 50 nM enzyme, 80 nM RNA and 1.12 μM [methyl-$^3$H]-AdoMet under the same buffer conditions as (B) but in the absence of NaCl (C). All buffer conditions were assayed in the presence of 2 mM DTT and 5 U RNasin®. All data points and standard deviations are from duplicate measurements.

Certain recombinant proteins have a tendency to aggregate and thus the effect of the neutral detergent, CHAPS was investigated. We observed that 0.05% (w/v) CHAPS augmented enzyme activity from pH 8 to 10 (Fig. 2B). The levels of increase were comparable to the effects observed for 10 mM KCl (Fig. 2B). To further study if combining the various salts and detergent had a synergistic effect on DENV2 MTase activity, the enzyme was assayed with buffers from pH 6 to 10 containing all the components. Interestingly, enzyme activity was enhanced from pH 7 to 8.5 with the highest levels achieved at pH 7–8 (Fig. 2B). In subsequent experiments and for inhibitor testing, the final assay buffer contained 50 mM Tris/HCl, pH 7 with 10 mM KCl, 2 mM $MgCl_2$ and 2 mM $MnCl_2$. To facilitate large-scale screening of compounds which are mainly hydrophobic, 0.05% CHAPS was also added to the final buffer.

We also sought to determine the effect of ionic salt concentration on DENV2 MTase (Fig. 2C). When NaCl was added to the final assay buffer at 2, 10 and 50 mM concentrations, there was negligible effect on enzymatic activity. Above 100 mM NaCl, there was a steady decline in enzymatic activity. At 300 mM NaCl, MTase activity was almost complete abolished. Consequently, this concentration of NaCl was included in the 2× stop buffer to terminate the enzyme reaction.

To study the effect of temperature on the activity of DENV2 MTase, we carried out the experiments at 22 °C (or room temperature), 30 or 37 °C using the final assay buffer conditions and monitored the reaction over 2 h. We observed that the activity of the enzyme was inversely proportional to the incubation temperature (Fig. 2D). Its catalytic activity was highest at room temperature and increased steadily over the 2-h incubation period. In addition, the rate of increase was linear up during the first 30 min and progressively declined over the next 1.5 h. When incubated at 30 °C, the enzyme was significantly less active and the rate of increase plateaued after 20 min. At 37 °C, the enzyme was completely inactive. These findings suggest that DENV MTase has an optimal temperature at 22 °C and higher temperatures may either prevent the enzyme from forming stable complexes with its RNA

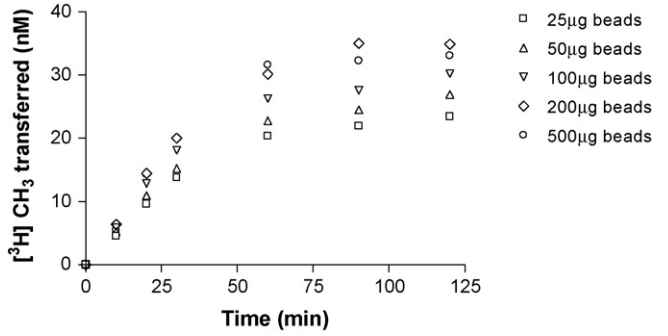


**Fig. 3.** Determination of optimal amounts of streptavidin–SPA beads for DENV2 MTase activity. 25 nM of MTase was incubated with 40 nM RNA substrate and 0.56 μM [methyl-$^3$H]-AdoMet in assay buffer (50 mM Tris/HCl pH 7, 10 mM KCl, 2 mM $MgCl_2$, 2 mM $MnCl_2$, 0.05% CHAPS, 2 mM DTT and 5 U RNasin®) at RT for a period of 2 h. At the indicated times, reaction was stopped with 2× stop buffer containing 25, 50, 100, 200 and 500 μg of SPA beads. All data points and standard deviations are from duplicate measurements.

substrate or perhaps induce irreversible denaturation of the protein. Data from thermal denaturation experiments revealed that the melting temperature of DENV MTase is about 40 °C (Supplementary Fig. 2). Hence, it is likely that loss of enzyme activity at 37 °C is due to both reasons. All subsequent experiments were performed at 22 °C.

### 3.2. Determination of optimal amount of streptavidin–SPA beads for methylation assay

The amount of streptavidin–SPA beads was varied at 25, 50, 100, 200, 500 μg to determine the optimal amount of beads that would bind methylated RNA and give the best reading. The amounts corresponded to a binding capacity of 2.5–5, 5–10, 10–20, 20–40 and 50–100 pmoles of $^3$H respectively. The reaction was set up as before and conducted over a period of 2 h at room temperature. The results showed that in all cases the reactions were linear from 0 to 30 min and that using 200 μg of SPA beads produced the highest signals (Fig. 3). No increase in signal was observed with addition of 500 μg of beads in the reaction. However, after 20 min, the best signal-to-noise levels were obtained with 100 μg of beads (13.6-fold over background) rather than with 200 μg beads (7.4-fold over background). This is because increasing the amount of SPA beads in the reaction increased the background noise proportionally. In our subsequent experiments, we used 100 μg of streptavidin–SPA beads to capture the biotinylated RNA substrate.

### 3.3. Linearity of methylation with respect to enzyme concentration and reaction time

We first performed methylation experiments to determine the linearity of product formation with respect to enzyme concentration. An increasing concentration of DENV2 MTase was added to fixed amounts of [methyl-$^3$H]-AdoMet and RNA substrate. The reaction was allowed to proceed for 20 min and the product formation was measured. We observed that the reaction was linear up to an enzyme concentration of 50 nM with a maximum of about 25 nM RNA methylated (Fig. 4A). At higher enzyme concentrations, the levels of methylation declined gradually. This indicates that only 62.5% of the input RNA substrate was methylated and suggests at higher enzyme concentrations, some substrate inhibition occurred, probably due to the formation of non-productive binary enzyme–AdoMet or enzyme–RNA complexes. However, it is also possible that product inhibition may have occurred since the product of the reaction, SAH is a potent inhibitor. Based on this data, the amount of enzyme was kept at 25 nM for subsequent experiments, to ensure that it falls

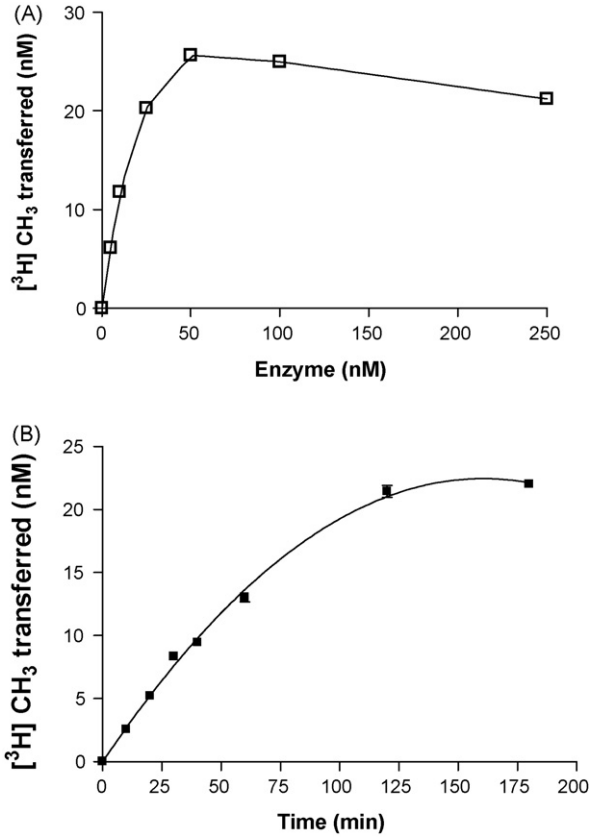


**Fig. 4.** Determination of linearity of methylation catalysed DENV2 MTase. Linearity of reaction as a function of enzyme concentration (A). Increasing concentrations of DENV2 MTase from 0 to 500 nM was incubated with 40 nM RNA substrate and 0.56 μM [methyl-$^3$H]-AdoMet (open square) or 80 nM RNA substrate and 1.12 μM [methyl-$^3$H]-AdoMet (open triangle), in assay buffer (50 mM Tris/HCl pH 7, 10 mM KCl, 2 mM $MgCl_2$, 2 mM $MnCl_2$, 0.05% CHAPS, 2 mM DTT and 5 U RNasin®) at RT for a period of 20 min. At the indicated times, reaction was stopped with 2× stop buffer containing 100 μg of SPA beads. Linearity of reaction as a function of time. 25 nM DENV2 MTase was incubated with 40 nM RNA substrate and 0.56 μM [methyl-$^3$H]-AdoMet in the same buffer conditions as (A) for a period of 3 h at RT (B). Both graphs are plotted as levels of [methyl-$^3$H] incorporated into the RNA template versus enzyme concentration (A) or time (B). All data points and standard deviations are from duplicate measurements.

within the linear range. We then investigated the linearity of product formation with respect to time and to ascertain if any product inhibition occurred. 25 nM enzyme was incubated with RNA substrate and [methyl-3H]-AdoMet as before and the reaction carried out at room temperature for 3 h. The progress curve was found to be linear up to 1 h and reached a plateau after 2 h (Fig. 4B). We noted that the maximum amount of methylated RNA formed was also less than the total amount of input RNA (about 20 nM), suggesting that some product inhibition occurred in this assay condition after 1 h. The result obtained here is comparable to those obtained in Fig. 2A and B. Therefore, for subsequent assay development and compound testing, the reaction time was maintained at 20 min with 25 nM enzyme to keep the amount of product formed to about 10% of the total substrate concentration. This also ensured that we are measuring the initial velocities in the enzyme catalyzed reactions (Copeland, 2000).

### 3.4. Steady-state kinetic parameters of DENV2 MTase on RNA substrate and AdoMet

To better understand the catalytic efficiency of DENV2 MTase with respect to RNA substrate and AdoMet under our estab-

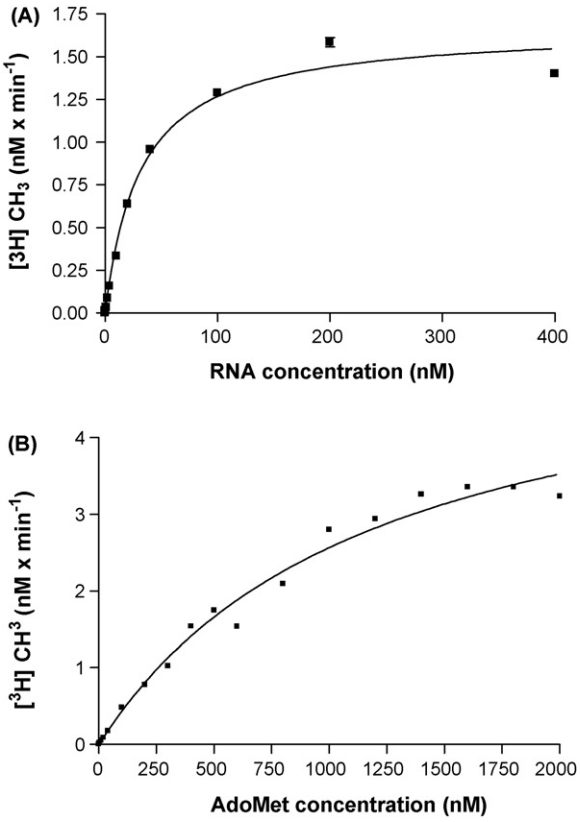


**Fig. 5.** Determination of steady-state kinetic parameters of DENV2 MTase. 25 nM DENV2 MTase was incubated in assay buffer (50 mM Tris/HCl pH 7, 10 mM KCl, 2 mM $MgCl_2$, 2 mM $MnCl_2$, 0.05% CHAPS, 2 mM DTT and 5 U RNasin®) at RT for a period of 20 min with (A) 0.95 μM [methyl-$^3$H]-AdoMet and increasing concentrations of RNA ranging from 0 to 0.4 μM or (B) 2 μM RNA and increasing concentrations of [methyl-$^3$H]-AdoMet ranging from 0 to 1 μM. The initial velocities of the reactions were plotted against the substrate concentrations and the steady-state parameters were obtained by a linear regression curve fitting as described in Section 2. Steady-state parameters obtained respectively for AdoMet and RNA were: $V_{max} = 3.71 \pm 0.01$ and $1.67 \pm 0.04$ nM min$^{-1}$; $K_m^{app} = 1194 \pm 187.8$ and $31.77 \pm 2.84$ nM; $k_{cat} = 2.47 \times 10^{-3}$ and $1.11 \times 10^{-3}$ s$^{-1}$; $k_{cat}/K_m = 2.07 \times 10^3$ and $34.7 \times 10^3$ M$^{-1}$ s$^{-1}$.

lished *in vitro* conditions, we performed experiments to study the enzyme activity under steady-state conditions. MTase activity was measured in the presence of a constant concentration enzyme and a saturating concentration of [methyl-$^3$H]-AdoMet and varying concentrations of RNA or a saturating concentration of RNA and varying concentrations of [methyl-$^3$H]-AdoMet. Reaction results were curve fitted according to one site binding mode (Michaelis–Menten curve; Eq. (1)) and plotted with reaction velocities as a function of RNA (Fig. 5A) or AdoMet (Fig. 5B) concentrations. Methylation saturation was obtained above 100 nM of RNA (Fig. 5A) and 1 μM AdoMet (Fig. 5B). Kinetic parameters $K_m^{app}$, and $V_{max}^{app}$ were obtained using nonlinear regression curve fitting and used to calculate the value for $k_{cat}^{app}$ (corresponding to the ratio of $V_{max}^{app}$ to enzyme concentration used) and the catalytic efficiency of the enzyme (see legend to Fig. 5). The very high affinity of DENV MTase for its RNA substrate ($K_m = 31.77 \pm 2.84$ nM) coupled with a low turnover ($k_{cat} = 1.11 \times 10^{-3}$ s$^{-1}$) is similar to that observed for vaccinia virus 2′-*O*-MTase (Barbosa and Moss, 1978; Lockless et al., 1998) and several DNA methyltransferases from human and bacteria including EcoP15I (Ahmad and Rao, 1994) and EcaI (Szilák et al., 1993) and KpnI (Bheemanaik et al., 2003) which acts on specific DNA sequences. These characteristics of DENV MTase likely reflects the nature of the capping function of this enzyme and are in line with previous observations that Flavivirus MTases only methylate RNA sequences with AG at the 5′ end (Dong et al., 2007; Egloff et al., 2007). Strong binding to N-terminal nucleotides in the 5′ UTR is necessary to facilitate efficient N7 and 2′-*O* methylations so as to prevent degradation of the viral RNA by cytoplasmic nucleases. On the other hand, a low enzyme turnover may help to recruit host factors which are needed for viral RNA transcription and/or translation. Finally, since only two methylation events occur per RNA template during viral RNA synthesis, it may not be critical to have a high enzymatic turnover rate.

### 3.5. Determination of methylation positions on RNA substrate

Recently, it has been shown the Flavivirus MTases possess both N7- and 2′-*O*-MTase activities (Ray et al., 2006) and that 2′-*O*-MTase activity occurs in the presence of short RNA templates (Egloff et al., 2002, 2007; Benarroch et al., 2004; Dong et al., 2007). To confirm that the current *in vitro* assay conditions with DENV2 MTase resulted in 2′-*O* methylation of the RNA substrate, we performed the following sets of experiments. Firstly, we incubated the RNA substrate with DENV2 MTase and [$^3$H-methyl]-AdoMet as before and then removed the GTP-cap from the RNA using TAP. We observed that the amounts of [$^3$H-methyl] incorporated in RNA substrate treated with TAP were similar to those in untreated RNA sample (Fig. 6A). This indicates that no [$^3$H-methyl] group had been added to the RNA GTP-cap. Secondly, we methylated the GTP-cap in the RNA substrate with vaccinia virus N7-MTase and cold AdoMet and then treated the RNA sample with DENV2 MTase and [$^3$H-methyl]-AdoMet as before (Fig. 6A). We compared the total amount of [$^3$H-methyl] incorporated in this sample with a control RNA substrate that was not pre-methylated with vaccinia virus N7-MTase. No significant difference was found between both samples, indicating again that no N7-MTase activity had taken place with DENV2 MTase (Fig. 6A). Finally, we further incubated the RNA substrate with both vaccinia virus N7- and 2′-*O*-MTases, or either of these enzymes separately in the presence of cold AdoMet for 2 h. After purification, the RNA was further methylated with DENV2 MTase and [$^3$H-methyl]-AdoMet. As a control, we used DENV2 MTase to methylate the RNA template without prior treatment with vaccinia virus MTases. Significant incorporation of [$^3$H-methyl] was observed in samples pre-treated with vaccinia virus N7-MTase and the levels were 45% higher than the control samples which were not pre-incubated with vaccinia virus enzymes (Fig. 6B). This suggests that the N7-GTP-capped RNA is a better substrate than GTP-capped RNA for the 2′-*O* activity of DENV2 MTase and is in agreement with the observation that N7-MTase activity precedes 2′-*O* activity (Dong et al., 2007). In contrast, we observed very little incorporation of [$^3$H-methyl] to RNA samples pre-treated with either vaccinia virus 2′-*O*-MTase alone or N7- and 2′-*O*-MTases (Fig. 6B). This data confirms that DENV2 MTase is only exhibiting 2′-*O* activity with the short RNA substrate under our assay conditions.

### 3.6. Pre-incubation studies with DENV2 MTase

DENV2 MTase is a bi-substrate enzyme and binding of AdoMet or RNA could occur in a random or sequential order. To understand the events of enzyme substrate association and the effects on catalytic competency of the binary complexes, recombinant MTase was pre-incubated with AdoMet or RNA for 10 min at RT, and the reaction initiated with addition of the missing component, RNA or AdoMet, respectively. As a control, AdoMet and RNA were similarly incubated and the reaction initiated with enzyme addition. The order of substrate addition did not appear to have a significant influence on the pre-steady-state methylation (Fig. 7). Addition of either AdoMet or RNA resulted in similar rates in enzymatic activity over the 1-h period. The levels of methylation were also

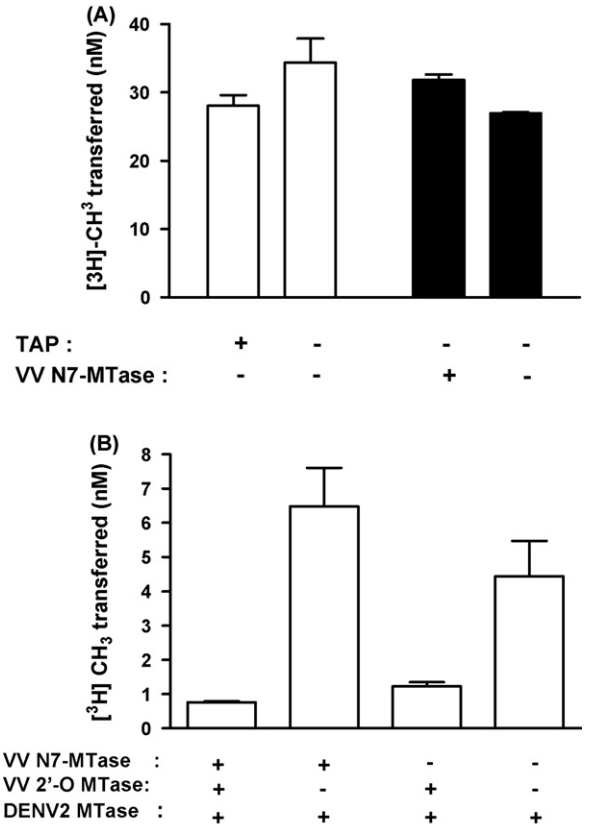


**Fig. 6.** Determination of methylation position on RNA template. RNA template was first incubated with DENV2 MTase and [methyl-$^3$H]-AdoMet for 1 h after which half of the reaction sample was treated with TAP and the amount of [methyl-$^3$H] incorporated into the RNA template was compared against the untreated sample (open bars; A). Secondly, RNA template was treated with vaccinia virus N7-MTase and cold AdoMet after which it was incubated with DENV2 MTase and [methyl-$^3$H]-AdoMet for 1 h (black bars, A). The amount of [methyl-$^3$H] incorporated into the RNA template was compared against a control RNA sample that was not pre-treated with vaccinia virus N7-MTase (black bars, A). In the third experiment, RNA template was pre-treated with both vaccinia virus N7- and 2′-*O*-MTases (first bar), N7-MTase (second bar) or 2′-*O*-MTase (third bar) alone and cold AdoMet for 2 h after which it was incubated with DENV2 MTase and [methyl-$^3$H]-AdoMet for 1 h (B). Control RNA sample was carried out without prior treatment with vaccinia virus MTases (fourth bar, B). All data points and standard deviations are from duplicate measurements.

comparable to the control reaction. This indicates that substrate binding of DENV2 MTase occurs in a rapid-equilibrium, random bi bi reaction. This characteristic is also found in all known cytosine methyltransferases studied so far, such as HhaI (Vilkaitis et al., 2001), murine DNMT1 (Flynn and Reich, 1998), human DNMT1, mammalian DNMT3 (Yokochi and Robertson, 2002) as well as in vaccinia virus 2′-*O*-MTase (Barbosa and Moss, 1978). Furthermore, the two binary complexes, enzyme–AdoMet or enzyme–RNA were equally efficient kinetically as they showed similar rates of methylation. Since the activities of the preformed catalytically competent binary complexes were not significantly different from the control, this also suggests that the enzyme binds both RNA and AdoMet with very high affinities. The results here are very different from observations of the interactions of host methyltransferases with AdoMet and their substrates. KpnI (Bheemanaik et al., 2003), G9a (Patnaik et al., 2004), T4 Dam (Malygin et al., 2004) form catalytically active complexes with AdoMet but not with their corresponding peptide/DNA substrates. EcoRV MTase–DNA complex was also reported to be inactive, whereas the enzyme–AdoMet was active (Gowher and Jeltsch, 2000). A GTP-binding pocket at the N-terminal of DENV2 MTase was postulated to be the binding site of RNA cap (Egloff et al., 2002). It is possible that the presence of this pocket contributed to the better catalytic competence of the DENV MTase–RNA complex.

### 3.7. Validation of methylation assay with compound testing

To assess the inhibitory potential of compounds against DENV2 MTase, the enzyme was first tested against the product of its reaction, *S*-adenosyl-homocysteine (SAH), which has been reported to be a potent competitive inhibitor of methyl-transferases (Bheemanaik et al., 2003; Patnaik et al., 2004). We further evaluated two natural products which bear structural similarity to AdoMet, sinefungin (Smith and Norton, 1980; Chrebet et al., 2005) and dehydrosinefungin (Smith and Norton, 1980). In addition, GTP and five GTP-based RNA cap analogues were also tested. DENV2 MTase was pre-incubated with increasing concentrations of inhibitor for 30 min, followed by initiation of reaction with [$^3$H]-AdoMet. Dose response curves indicated that SAH was very potent against DENV2 MTase, with $IC_{50}$ value of $0.62 \pm 0.03$ μM (Fig. 8, Table 1). Sinefungin was equally potent whilst dehydrosinefungin was about 3-fold less active (Fig. 8, Table 1). $IC_{50}$ value for sinefungin obtained here deviates significantly from that obtained for WNV MTase (14 μM;

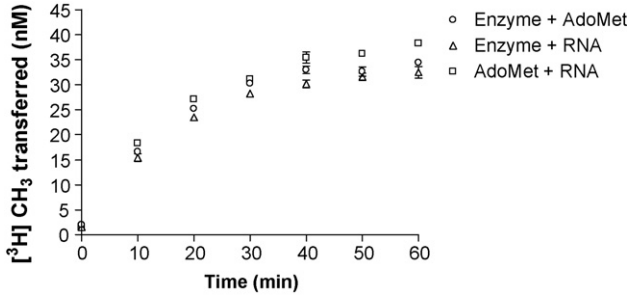


**Fig. 7.** Re-incubation analysis of DENV2 MTase. Methylation reactions were performed in assay buffer (50 mM Tris/HCl pH 7, 10 mM KCl, 2 mM $MgCl_2$, 2 mM $MnCl_2$, 0.05% CHAPS, 2 mM DTT and 5 U RNasin®) at RT for a period of 1 h with 20 nM enzyme, 40 nM RNA template and 0.56 μM [methyl-$^3$H]-AdoMet. Reaction was started by the addition of RNA to a solution containing enzyme and AdoMet (open circle), addition of AdoMet to a solution containing enzyme and RNA (open triangle), or addition of enzyme to a solution containing RNA and AdoMet (open square). All data points and standard deviations are from duplicate measurements.

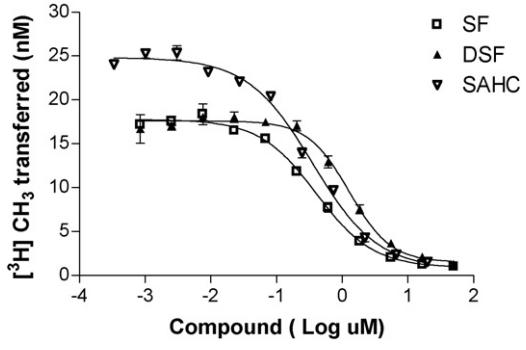


**Fig. 8.** Inhibitory effects of competitive inhibitors against DENV2 MTase. Methylation reactions were determined with DENV2 MTase in assay buffer (50 mM Tris/HCl pH 7, 10 mM KCl, 2 mM $MgCl_2$, 2 mM $MnCl_2$, 0.05% CHAPS, 2 mM DTT and 5 U RNasin®) at room temperature for a period of 20 min with 20 nM enzyme, 40 nM RNA template and 0.56 μM [methyl-$^3$H]-AdoMet and increasing concentrations of sinefungin (open square), dehydrosinefungin (filled triangle) and SAH (inverted triangle), ranging from 0 to 20 μM. Plots of [methyl-$^3$H] levels incorporated into the RNA template versus logarithm of compound concentration was used to determine the concentration of compound needed to inhibit 50% of the enzyme activity.

**Table 1**
Inhibition of DENV2 MTase activity by competitive inhibitors (*S*-adenosylhomocysteine, sinefungin and dehydrosinefungin) and GTP-pocket binders (GTP, RNA cap analogues).

| Compounds | Average $IC_{50}$ (μM) | No. of experiments | *Z′* factor |
|---|---|---|---|
| SAHC | 0.62 ± 0.04 | 3 | 0.80–0.98 |
| Sinefungin | 0.42 ± 0.14 | 4 | 0.77–0.93 |
| Dehydrosinefungin | 1.28 ± 0.12 | 4 | 0.60–0.83 |
| GTP | 228.6 ± 43.4 | 4 | 0.72–0.89 |
| G[5′]ppp[5′]A | 151.4 ± 23.8 | 4 | 0.60–0.77 |
| $m^7$G[5′]ppp[5′]A | 144.6 ± 21.0 | 4 | 0.60–0.77 |
| $m_2{}^{7,3'\text{-}O}$G[5′]ppp[5′]G | 310.6 ± 36.8 | 2 | 0.60–0.69 |
| $m_2{}^{2,2,7}$G[5′]ppp[5′]G | 399.6 ± 87.6 | 2 | 0.60–0.72 |
| $m^7$G[5′]ppp[5′]$m^7$G | 83.0 ± 9.4 | 3 | 0.60–0.77 |

The results shown are the average of two to four independent experiments and the average *Z′* factor obtained was ≥0.6.

Dong et al., 2008). We speculate that the difference is due to the TLC plate-based assay which is less sensitive than SPA-based method.

We observed that the inhibitory activity of GTP was relatively poor ($IC_{50}$ = 228.6 ± 43.4 μM; Table 1) but was improved almost 2-fold by linking two ribonucleotides as a G[5′]ppp[5′]A cap analogue (Table 1). There was very little difference in the inhibitory activity between G[5′]ppp[5′]A and mono-N7-methylated G[5′]ppp[5′]A (Table 1) but binding of a 2-way methylated structure, $m^7$G[5′]ppp[5′]$m^7$G improved activity by 2-fold (Table 1). On the other hand, two other hyper-methylated forms of the RNA cap analogue, $m_2{}^{7,3'\text{-}O}$G[5′]ppp[5′]G and $m_2{}^{2,2,7}$G[5′]ppp[5′]G were much less potent than GTP (Table 1). Overall, the data suggests that the affinity of GTP for the cap-binding pocket in DENV2 MTase is poorer than RNA cap structures. These results contradict those of Egloff et al. (2007) who reported $K_d$ of GTP and G[5′]ppp[5′]G were similar (58 and 65 μM, respectively), whilst that of $m^7$GpppG was 255 ± 5 μM. In subsequent reports, GTP was found to inhibit DENV2 (Egloff et al., 2007) and WNV (Dong et al., 2008) MTases with $IC_{50}$ values of 0.34 mM and 0.1 mM respectively, whilst $m^7$G[5′]ppp[5′]A inhibited these enzymes with $IC_{50}$ values of 1.7–2.5 and 5 mM. The reason for these differences is unknown, but may be attributed to the different assay formats used. To further study the interaction of the GTP and RNA cap analogues with DENV2 MTase, we performed thermal denaturation experiments to assess their effects on MTase stability by using the fluorescence dye, SyproOrange (Supplementary Fig. 2). We observed that binding of G[5′]ppp[5′]A and $m^7$G[5′]ppp[5′]A stabilized MTase more than GTP as both cap analogues increased the melting temperature ($T_m$) of DENV2 MTase more than GTP. Similar to the inhibition curves of the RNA cap analogues observed in the enzymatic assay, $m^7$G[5′]ppp[5′]$m^7$G induced the greatest increase in $T_m$ of the protein, whilst $m_2{}^{2,2,7}$G[5′]ppp[5′]G did not cause any change.

## 4. Conclusions

This report describes the development of a simple, rapid and sensitive scintillation proximity assay to detect dengue virus 2′-*O*-MTase activity. Both monovalent and divalent cations increased its catalytic activity, with the latter resulting in dramatic enhancement and a shift in pH maximal to near physiological conditions. Preliminary testing with inhibitors showed that the assay consistently produced good *Z′* factor values (≥0.6) and is therefore suitable for high-throughput screening of compounds. Biochemical characterization indicates that this enzyme displays a very high affinity for its RNA substrate compared to AdoMet and turnover of both substrates is relatively low. Overall, its catalytic profile is akin to vaccinia virus 2′-*O*-MTase and other sequence-specific DNA methyltransferases which have been previously studied and is the first detailed biochemical analysis of a Flavivirus methyltransferase.

## Acknowledgments

We wish to thank Chen Yen Liang for design of the RNA substrate and Esther Schmidtt (Novartis Institutes for Biomedical Research, Basel) for providing dehydrosinefungin. We are grateful to Christophe Bodenreider for critical review of the manuscript and David Beer for useful suggestions.

## Appendix A. Supplementary data

Supplementary data associated with this article can be found, in the online version, at doi:10.1016/j.antiviral.2008.08.005.

## References

Ahmad, I., Rao, D.N., 1994. Interaction of EcoP15I DNA methyltransferase with oligonucleotides containing the asymmetric sequence 5′-CAGCAG-3′. J. Mol. Biol. 242, 378–388.
Barbosa, E., Moss, B., 1978. mRNA (nucleoside-2′-)-methyltransferase from vaccinia virus. J. Biol. Chem. 253, 7698–7702.
Benarroch, D., Egloff, M.P., Mulard, L., Guerreiro, C., Romette, J.L., Canard, B., 2004. A structural basis for the inhibition of the NS5 dengue virus mRNA 2′-*O*-methyltransferase domain by ribavirin 5′-triphosphate. J. Biol. Chem. 279, 35638–35643.
Bheemanaik, S., Chandrashekaran, S., Nagaraja, D., Rao, D.N., 2003. Kinetic and catalytic properties of dimeric KpnI DNA methyltransferase. J. Biol. Chem. 278, 7863–7874.
Chambers, T.J., Hahn, C.S., Galler, R., Rice, C.M., 1990. Flavivirus genome organization, expression, and replication. Annu. Rev. Microbiol. 44, 649–688.
Chrebet, G.L., Wisniewski, D., Perkins, A.L., Deng, Q., Kurtz, M.B., Marcy, A., Parent, S.A., 2005. Cell-based assays to detect inhibitors of fungal mRNA capping enzymes and characterization of sinefungin as a cap methyltransferase inhibitor. J. Biomol. Screen. 10, 355–364.
Cleaves, G.R., Dubin, D.T., 1979. Methylation status of intracellular dengue type 2 40 S RNA. Virology 96, 159–165.
Copeland, R.A., 2000. Enzymes: A Practical Introduction to Structure, Mechanism and Data Analysis. John Wiley and Sons Inc., New York.
Dong, H., Ray, D., Ren, S., Zhang, B., Puig-Basagoiti, F., Takagi, Y., Ho, C.K., Li, H., Shi, P.Y., 2007. Distinct RNA elements confer specificity to flavivirus RNA cap methylation events. J. Virol. 81, 4412–4421.
Dong, H., Ren, S., Zhang, B., Zhou, Y., Puig-Basagoiti, F., Li, H., Shi, P.Y., 2008. West Nile virus methyltransferase catalyzes two methylations of the viral RNA cap through a substrate-repositioning mechanism. J. Virol. 82, 4295–4307.
Egloff, M.P., Benarroch, D., Selisko, B., Romette, J.L., Canard, B., 2002. An RNA cap (nucleoside-2′-*O*-)-methyltransferase in the flavivirus RNA polymerase NS5: crystal structure and functional characterization. EMBO J. 21, 2757–2768.
Egloff, M.P., Decroly, E., Malet, D.H., Selisko, B., Benarroch, D., Ferron, F., Canard, B., 2007. Structural and functional analysis of methylation and 5′-RNA sequence requirements of short capped RNAs by the methyltransferase domain of dengue virus NS5. J. Mol. Biol. 372, 723–736.
Finney, D.J., 1976. Radioligand assay. Biometrics 32, 721–740.
Flynn, J., Reich, N., 1998. Murine DNA (cytosine-5-)-methyltransferase: steady-state and substrate trapping analyses of the kinetic mechanism. Biochemistry 37, 15162–15169.
Furuichi, Y., Shatkin, A.J., 2000. Viral and cellular mRNA capping: past and prospects. Adv. Virus Res. 55, 135–184.
Ghosh, A.K., Liu, W., 1997. A convergent enantioselective total synthesis of streptogramin antibiotic (−)-Madumycin II. J. Org. Chem. 62, 7908–7909.
Gowher, H., Jeltsch, A., 2000. Molecular enzymology of the EcoRV DNA-(adenine-N(6))-methyltransferase: kinetics of DNA binding and bending, kinetic mechanism and linear diffusion of the enzyme on DNA. J. Mol. Biol. 303, 93–110.
Gu, M., Lima, C.D., 2005. Processing the message: structural insights into capping and decapping mRNA. Curr. Opin. Struct. Biol. 15, 99–106.
Gubler, D.J., 1998. Dengue and dengue hemorrhagic fever. Clin. Microbiol. Rev. 11, 480–496.
Koonin, E.V., 1993. Computer-assisted identification of a putative methyltransferase domain in NS5 protein of flaviviruses and λ2 protein of reoviruses. J. Appl. Crystallogr. 24, 946–950.
Kroschewski, H., Lim, S.P., Butcher, R.E., Yap, T.L., Lescar, J., Wright, P.J., Vasudevan, S.G., Davidson, A.D., 2008. Mutagenesis of the dengue virus type 2 NS5 methyltransferase domain. J. Biol. Chem. 283, 19410–19421.
Li, C., Gershon, P.D., 2006. p$K_a$ of the mRNA cap-specific 2′-*O*-methyltransferase catalytic lysine by HSQC NMR detection of a two-carbon probe. Biochemistry 45, 907–917.
Li, H., Clum, S., You, S., Ebner, K.E., Padmanabhan, R., 1999. The serine protease and RNA-stimulated nucleoside triphosphatase and RNA helicase functional

domains of dengue virus type 2 NS3 converge within a region of 20 amino acids. J. Virol. 73, 3108–3116.
Lindenbach, B.D., Rice, C.M., 2001. Flaviviridae: the viruses and their replication. In: Howley, P.M. (Ed.), Fields Virology, vol. 1, 4th ed. Lippincott Williams & Williams, Philadelphia, PA, pp. 991–1042.
Lockless, S.W., Cheng, H.T., Hodel, A.E., Quiocho, F.A., Gershon, P.D., 1998. Recognition of capped RNA substrates by VP39, the vaccinia virus-encoded mRNA cap-specific 2′-*O*-methyltransferase. Biochemistry 37, 8564–8574.
Luzhkov, V.B., Selisko, B., Nordqvist, A., Peyrane, F., Decroly, E., Alvarez, K., Karlen, A., Canard, B., Qvist, J., 2007. Virtual screening and bioassay study of novel inhibitors for dengue virus mRNA cap (nucleoside-2′O)-methyltransferase. Bioorg. Med. Chem. 15, 7795–7802.
Malygin, E.G., Sclavi, B., Zinoviev, V.V., Evdokimov, A.A., Hattman, S., Buckle, M., 2004. Bacteriophage T4Dam DNA-(adenine-N(6))-methyltransferase. Comparison of pre-steady state and single turnover methylation of 40-mer duplexes containing two (un)modified target sites. J. Biol. Chem. 279, 50012–50018.
Mao, X., Schwer, B., Shuman, S., 1995. Yeast mRNA cap methyltransferase is a 50-kilodalton protein encoded by an essential gene. Mol. Cell. Biol. 15, 4167–4174.
Ogino, T., Kobayashi, M., Iwama, M., Mizumoto, K., 2005. Sendai virus RNA-dependent RNA polymerase L protein catalyzes cap methylation of virus-specific mRNA. J. Biol. Chem. 280, 4429–4435.
Patnaik, D., Chin, H.G., Estève, P.O., Benner, J., Jacobsen, S.E., Pradhan, S., 2004. Substrate specificity and kinetic mechanism of mammalian G9a histone H3 methyltransferase. J. Biol. Chem. 279, 53248–53258.
Pugh, C.S., Bochardt, R.T., Stone, H.O., 1978. Sinefungin, a potent inhibitor of virion mRNA(guanine-7-)-methyltransferase, mRNA(nucleoside-2′-)-methyltransferase, and viral multiplication. J. Biol. Chem. 253, 4075–4077.
Ray, D., Shah, A., Tilgner, M., Guo, Y., Zhao, Y., Dong, H., Deas, T.S., Zhou, Y., Li, H., Shi, P.Y., 2006. West Nile virus 5′-cap structure is formed by sequential guanine N-7 and ribose 2′-*O* methylations by nonstructural protein 5. J. Virol. 80, 8362–8370.
Rice, C.M., Lenches, E.M., Eddy, S.R., Shin, S.J., Sheets, R.L., Strauss, J.H., 1985. Nucleotide sequence of yellow fever virus: implications for flavivirus gene expression and evolution. Science 229, 726–733.
Rodbard, D., Hutt, D.M., 1974. Statistical analysis of radioimmunoassay, and immunoradiometirc (labeled antibody) assays: a generalized, weighted, iterative least-squares method for logistic curve fitting. In: Radioimmunoassay and Related Procedures in Medicine, vol. 1. Int. Aromic Energy Agency, Vienna, pp. 165–192.
Shuman, S., 2001. Structure, mechanism and evolution of the mRNA capping apparatus. Prog. Nucl. Acid Res. Mol. Biol. 66, 1–40.
Smith Jr., D.D., Norton, S.J., 1980. Inhibition of cyclopropane fatty acid synthase by sinefungin and A9145C. Biochem. Biophys. Res. Commun. 94, 1458–1462.
Szilák, L., Dér, A., Deák, F., Venetianer, P., 1993. Kinetic characterization of the EcaI methyltransferase. Eur. J. Biochem. 218, 727–733.
Vilkaitis, G., Merkiene, E., Serva, S., Weinhold, E., Klimasauskas, S., 2001. The mechanism of DNA cytosine-5 methylation. Kinetic and mutational dissection of Hhai methyltransferase. J. Biol. Chem. 276, 20924–20934.
Wengler, G., 1981. Terminal sequences of the genome and replicative-form RNA of the flavivirus West Nile virus: absence of poly(A) and possible roles in RNA replication. Virology 113, 544–555.
Wu, S., Liu, B., 2000. Application of scintillation proximity assay in drug discovery. BioDrugs 19, 383–392.
Yap, T.L., Xu, T., Chen, Y.L., Malet, H., Egloff, M.P., Canard, B., Vasudevan, S.G., Lescar, J., 2007. Crystal structure of the dengue virus RNA-dependent RNA polymerase catalytic domain at 1.85-angstrom resolution. J. Virol. 81, 4753–4765.
Yokochi, T., Robertson, K.D., 2002. Preferential methylation of unmethylated DNA by mammalian de novo DNA methyltransferase Dnmt3a. J. Biol. Chem. 277, 11735–11745.
Zhang, J., Chung, T.D.Y., Oldenburg, K.R., 1999. A simple statistical parameter for use in evaluation and validation of high throughput screening assays. J. Biomol. Screen. 4, 67–73.
Zhou, Y., Ray, D., Zhao, Y., Dong, H., Ren, S., Li, Z., Guo, Y., Bernard, K.A., Shi, P.Y., Li, H., 2007. Structure and function of flavivirus NS5 methyltransferase. J. Virol. 81, 3891–3903.